Benzyl-Substituted Tin Chalcogenides. Efficient Single-Source Precursors for Tin Sulfide, Tin Selenide, and $Sn(S_xSe_{1-x})$ Solid Solutions

Philip Boudjouk,* Dean J. Seidler, Dean Grier, and Gregory J. McCarthy

Center for Main Group Chemistry, Department of Chemistry, North Dakota State University, Fargo, North Dakota 58105

Received September 19, 1995. Revised Manuscript Received March 18, 1996[⊗]

The benzyl-substituted tin chalcogenides $(Bn_3Sn)_2S$ (**1**), $(Bn_2SnS)_3$ (**2**), $(Bn_3Sn)_2Se$ (**3**), and $(Bn_2SnSe)_3$ (**4**), prepared from the corresponding benzyltin chloride and anhydrous sodium chalcogenide in THF, are convenient single-source precursors for tin sulfide or tin selenide. Pyrolysis (450 °C) of these precursors gave gray or black powders and bibenzyl as the major products. X-ray diffraction (XRD) analysis of the powders from the linear compounds **1** and **3** showed that SnS and SnSe were produced along with elemental tin, as expected from the precursor stoichiometry. In contrast, the solids generated by cyclics **2** and **4** contained only SnS and SnSe respectively. Solid solutions of the formula $Sn(S_xSe_{1-x})$ were prepared by heating mixtures of **2** and **4**. The value of x could be controlled by varying the ratio of **2** to **4**. Combustion analysis showed less than 1% residual carbon in all tin sulfide and tin selenide samples.

Introduction

The orthorhombic forms of tin sulfide (SnS) and tin selenide (SnSe) are classified as narrow-bandgap semiconductors and therefore have the potential to serve as efficient materials in photovoltaic applications. Tin(II) sulfide possesses an optical bandgap of 1.08 eV, which is very close to that of silicon and is especially attractive due to its high conversion efficiency in photovoltaic devices (∼25%).[1,2] It also possesses favorable properties with respect to cost, availability, toxicity, and stability.[3] Photoelectric studies on films of tin(II) selenide indicate it shows similar promise in energy-conversion devices and may be useful in its polycrystalline form.[4] This would circumvent many of the difficulties associated with the deposition of epitaxial films necessary for the implementation of other semiconductors in this capacity. Polycrystalline films of SnSe have also found use in memory switching devices.[5] In light of these facts, it is rather surprising that relatively little attention has been paid to the synthesis of these materials in the literature.

The orthorhombic structures of group 14/16 solids are of crystallographic interest because they are intermediate between three-dimensional crystalline networks and two-dimensional layer type compounds.[6] Included in this class are SnS and SnSe.[7] SnS and SnSe are isomorphous and crystallize in the orthorhombic (*Pbnm*) [GeS] structure, as do their intermediates within the continuous solid solution $Sn(S_xSe_{1-x})$, $0 \le x \le 1$.[8] The [GeS] structure can be viewed as stacked double layers each consisting of puckered 6-membered rings, similar to the black phosphorus structure. Within these $Sn(S_xSe_{1-x})$ double layers, each tin atom is covalently bonded to three neighboring chalcogens, and each chalcogen atom is covalently bonded to three neighboring tin atoms.[9] The double layers, stacked along the *b* axis, are held together primarily by van der Waals forces.[10] This layered structure has been used to justify the description of the optical energy gap and other electrooptical properties of these compounds in terms of a strictly two-dimensional model.[11]

Structural studies of SnS and SnSe solid solutions showed that the unit-cell parameters varied linearly across the composition range.[9] This linear behavior has been observed in other metal sulfide/selenide solid solutions: Ge(S,Se) and Pb(S,Se).[12,13] Similar studies of the $CuIn(S,Se)_2$ solid solution series have shown only slight deviations from linearity in the unit-cell parameters.[14] Electrical and optical properties, such as hole mobility and optical bandgap, in Sn(S,Se) were found to vary in an orderly, but nonlinear, fashion as a function of

[⊗] Abstract published in *Advance ACS Abstracts,* May 1, 1996.

(1) (a) Singh, J. P.; Bedi, R. K. *Thin Solid Films* **1991**, *199*, 9. (b) Nair, M. T. S.; Nair, P. K. *Semicond. Sci. Technol.* **1991**, *6*, 132. (c) Rodot, M. *Acta Electron.* **1975**, *18*, 345. (d) Rodot, M. *Rev. Phys. Appl.* **1977**, *12*, 411. (d) Prince, M. B. *J. Appl. Phys.* **1955**, *26*, 534. (e) Loferski, J. J. *J. Appl. Phys.* **1956**, *27*, 777.
(2) Singh, J. P.; Bedi, R. K. *Thin Solid Films* **1991**, *199*, 9.
(3) Nair, M. T. S.; Nair, P. K. *Semiconduct. Sci. Technol.* **1991**, *6*, 132.
(4) Bennouna, A.; Tessier, P. Y.; Priol, M.; Dang Tran, Q.; Robin, S. *Phys. Status Solidi B* **1983**, *117*, 51.
(5) Subba Rao, T.; Samanata Ray, B. K.; Chaudhuri, A. K. *Thin Solid Films*, **1988**, *165*, 257.
(6) Logothetidid, S.; Polatoglou, H. M. *Phys. Rev. B* **1987**, *36*, 7491.
(7) Singh, J. P.; Bedi, R. K. *Thin Solid Films* **1991**, *199*, 9.
(8) Albers, W.; Haas, C.; Ober, H.; Schodder, G. R.; Wasscher, J. D. *J. Phys. Chem. Solids* **1962**, *23*, 215.
(9) Wiedemeier, H.; von Schnering, H. G. *Z. Kristallogr.* **1978**, *148*, 295.
(10) Taniguchi, M.; Johnson, P. L.; Ghijsen, J.; Cardona, M. *Phys. Rev. B* **1990**, *42*, 3634.
(11) Elkorashy, A. M. *Chemtronics* **1986**, *1*, 76.
(12) Koren, N. N.; Kindyak, V. V.; Matyas, E. E. *Phys. Status Solidi A* **1983**, *80*, K105.
(13) Strauss, A. J. *Trans. Metall. Soc. AIME* **1968**, *242*, 354.
(14) Landry, C. C.; Lockwood, J.; Barron, A. R. *Chem. Mater.* **1995**, *7*, 699.
(15) Pierson, H. O. *Handbook of Chemical Vapor Deposition (CVD): Principles, Technology and Applications*; Noyes Publications: Park Ridge, NJ, 1992.

S0897-4756(95)00434-0 CCC: $12.00

composition.[9] These considerations suggest that tailoring the physical, electrical, or optical properties of a material to specification by varying its composition in a controlled fashion is feasible.[15]

Recently we reported that pyrolyses of linear and cyclic perphenylated derivatives of tin chalcogenides, which proceed by a novel intramolecular phenyl migration mechanism, are efficient routes to SnS, SnSe, and SnTe.[16,17] In these cases, the phenyl groups migrate to form stable volatile byproducts such as tetraphenyltin and diphenyl sulfide, diphenyl selenide, or diphenyl telluride. We also discovered that mixtures of $(Ph_2SnS)_3$ and $(Ph_2SnSe)_3$ give high yields of solid solutions of $Sn(S_xSe_{1-x})$, $0 \le x \le 1$.[18] Low-temperature pyrolysis of perarylated systems such as Ph_2GaEPh_2, E = As, P also proved effective in preparing gallium arsenide and gallium phosphide.[19] The unexpected ease with which phenyl groups released metal chalcogenides led us to consider other less conventional groups in precursor design.

Benzyl-substituted derivatives of the main-group elements have not been investigated in depth, although, as Barron has shown, the absence of β hydrogens is a stabilizing factor for this class of compounds, as it is for transition-metal derivatives.[20] Comparison of the tin−organyl bond dissociation energies indicate that the largely ignored functional groups such as benzyl and allyl may serve as suitable leaving groups. Their dissociation energies are 163 ± 21 and 154 ± 21 kJ/mol, respectively. These values are relatively low when compared to those of methyl (230 ± 20 kJ/mol), ethyl (209 ± 20 kJ/mol), and isopropyl (209 ± 20 kJ/mol).[21] During the course of our studies, Chisholm published a synthesis of transition metal oxides from organometallic precursors containing a benzyl group.[22]

In this paper we present results clearly demonstrating the utility of the benzyl group in designing organometallic precursors to solid-state materials. Initially, we prepared the linear perbenzylated stannathianes and stannaselenanes (**1** and **3**) as the perbenzylated ana-

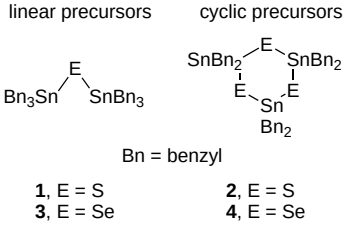

logues of the perphenylated precursors which we previously demonstrated can serve as convenient nonstoichiometric precursors to binary group 14/16 solid-state materials.[16,17] The phenyl-substituted compounds are described as nonstoichiometric precursors because the ratio of the metal to chalcogen found in the solid-state product differs from their ratio in the molecular starting material. Unlike the phenyl groups which undergo a series of migrations during the decomposition of the precursor, the benzyl groups in compounds **1** and **3** cleave homolytically, with all benzyl groups departing, to give high yields of tin sulfide and tin selenide, respectively, each intimately mixed with elemental tin. The cyclic precursors (**2** and **4**) proved to be atom efficient by generating only the target tin chalcogenide and bibenzyl. These results are consistent with a simple metal−carbon bond homolysis rather than a migration of the functional group. The loss of bibenzyl occurs under relatively mild (~210 °C) conditions for all the precursors investigated in this study. Unlike their phenyl analogues, these benzyl species are stoichiometric molecular precursors.

We describe below the synthesis of these perbenzylated precursors and a series of pyrolysis studies which show that they are not only good sources of tin sulfide and tin selenide but, when precursors **2** and **4** are combined and pyrolyzed, solid solutions of the formula $Sn(S_xSe_{1-x})$, $0 \le x \le 1$, are formed in good yields. We also demonstrate that the variable x can be controlled by manipulating the ratio of precursors in the initial mixture.

Results and Discussion

Synthesis of $(Bn_3Sn)_2E$ and $(Bn_2SnE)_3$ (E = S, Se). Combining anhydrous sodium sulfide and sodium selenide with Bn_3SnCl or Bn_2SnCl_2 in appropriate ratios produces the expected benzyl-substituted tin chalcogenides in very good yields (eqs 1 and 2). These

$$2Bn_3SnCl + Na_2E \rightarrow (Bn_3Sn)_2E + 2NaCl \quad (1)$$

1, E = S (78%)
3, E = Se (88%)

$$Bn_2SnCl_2 + Na_2E \rightarrow (Bn_2SnE)_3 + 2NaCl \quad (2)$$

2, E = S (85%)
4, E = Se (97%)

derivatives are air and moisture stable and can be isolated using a simple water/ether work up. The final products were crystallized from ether to give white, flaky solids.

Pyrolysis of $(Bn_3Sn)_2E$ and $(Bn_2SnE)_3$ (E = S, Se). The pyrolyses were carried out under an inert atmosphere of dry nitrogen. In all cases white crystalline solids deposited on the cooler portions of the pyrolysis tube while dark gray ceramic material remained in the crucible. The ceramic yields agreed very well with the calculated yields based on eqs 3 and 4. Bibenzyl was detected as the sole volatile byproduct. Mass recovery exceeded 90% in all cases.

$$(Bn_3Sn)_2E \rightarrow SnE + Sn + 3Bn{-}Bn\uparrow \quad (3)$$

1, E = S; ceramic yield of SnS + Sn: 32.7% (theoretical = 33.0%)
3, E = Se; ceramic yield of SnSe + Sn: 35.2% (theoretical = 36.7%)

$$(Bn_2SnE)_3 \rightarrow 3SnE + 3Bn{-}Bn\uparrow \quad (4)$$

2, E = S; ceramic yield of SnS: 44.6% (theoretical = 45.3%)
4, E = Se; ceramic yield of SnSe: 50.7% (theoretical = 52.1%)

(16) Boudjouk, P.; Bahr, S. R.; McCarthy, G. J. *Chem. Mater.* **1992**, *4*, 383.
(17) Boudjouk, P.; Seidler, D. J.; Bahr, S. R.; McCarthy, G. J. *Chem. Mater.* **1994**, *6*, 2108.
(18) Boudjouk, P.; Seidler, D. J.; Bahr, S. R.; Grier, D.; McCarthy, G. J., manuscript in preparation.
(19) Pan, Y.; Boudjouk, P. *Main Group Chem.* **1995**, *1*, 61.
(20) Barron, A. R. *J. Chem. Soc., Dalton Trans.* **1989**, 1625.
(21) Yergey, A. L.; Lampe, F. W. *Angew. Chem., Int. Ed. Engl.* **1969**, *81*, 296.
(22) Baxter, D. V.; Chisholm, M. H.; DiStasi, V. F.; Haubrich, S. T. *Chem. Mater.* **1995**, *7*, 84.

Table 1. Solid Solutions from Mixtures of Perbenzylated Ring Systems

composition of mixture of precursors	composition of solid solution[a]	isolated yield (%)	theoretical yield[b] (%)	% carbon
$3(Bn_2SnS)_3 + (Bn_2SnSe)_3$	$Sn(S_{0.75}Se_{0.25})$	48.1	47.0	0.55
$(Bn_2SnS)_3 + (Bn_2SnSe)_3$	$Sn(S_{0.50}Se_{0.50})$	48.1	49.0	0.50
$(Bn_2SnS)_3 + 3(Bn_2SnSe)_3$	$Sn(S_{0.25}Se_{0.75})$	51.1	50.4	0.51

[a] Theoretical composition based upon the ratio in which the cyclic precursors were combined before pyrolysis. [b] Theoretical yield is calculated assuming the loss of only the benzyl groups.

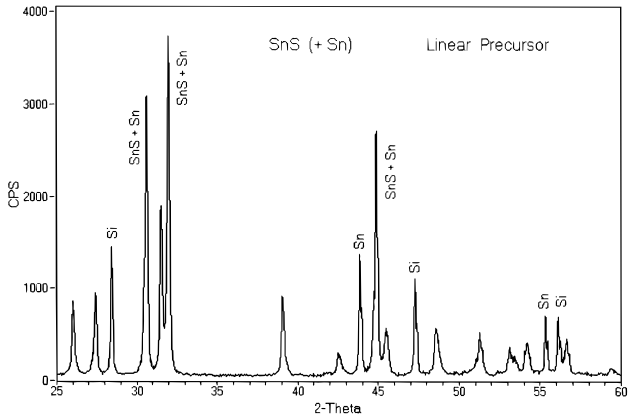

Figure 1. X-ray diffractogram of SnS and Sn prepared from the pyrolysis of $(Bn_3Sn)_2S$. Silicon used as an internal *d*-spacing standard. Unlabeled peaks due to SnS.

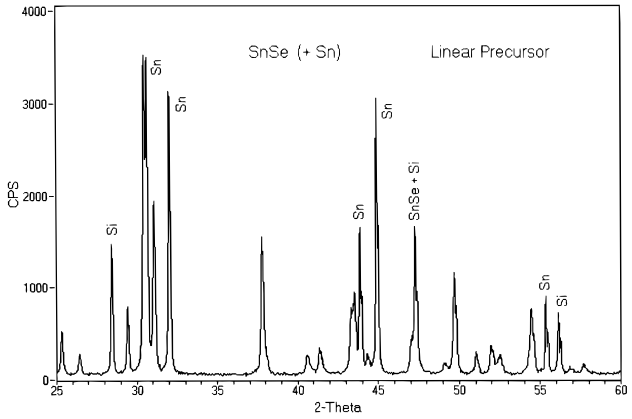

Figure 2. X-ray diffractogram of SnSe and Sn prepared from the pyrolysis of $(Bn_3Sn)_2Se$. Silicon used as an internal *d*-spacing standard. Unlabeled peaks due to SnSe.

The reaction of the precursors appears general and mixing of the cyclic precursors in 3:1, 1:1, and 1:3 molar ratios prior to pyrolysis resulted in the expected ceramic yields based upon the amount of each precursor present (Table 1). The carbon content in the ceramic remained low, less than 1%, while the hydrogen content was below the detection limit. This suggests the carbon may be present in its graphitic form rather than as a molecular residue.

X-ray Diffraction Analysis. Pyrolysis of the linear compounds $(Bn_3Sn)_2E$ (E = S, Se), produces an intimate mixture of the expected tin chalcogenide and elemental tin (eq 3), as determined by XRD (Figures 1 and 2). On the other hand, pyrolysis of the cyclic compounds, $(Bn_2SnE)_3$ (E = S, Se), gives only SnE and bibenzyl (Figures 3 and 4). Thus, in each case, the ratio of the elements recovered in the ceramic are consistent with the ratio present in the precursor molecule. The identity and phase purity of these products were determined by comparison of their X-ray diffractograms to those found in the ICDD Powder Diffraction File. All reflections in the diffractograms were accounted for by the binary

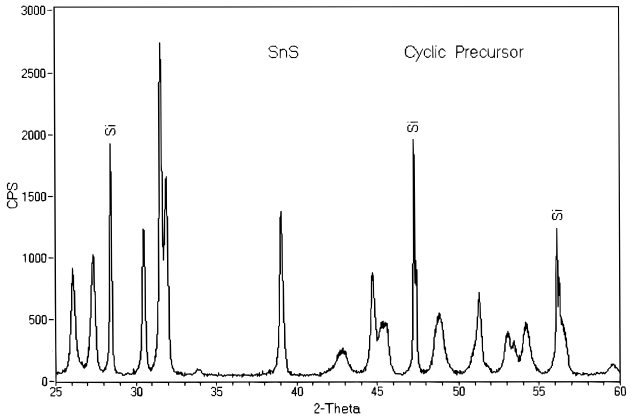

Figure 3. X-ray diffractogram of SnS prepared from the pyrolysis of $(Bn_2SnS)_3$. Silicon used as an internal *d*-spacing standard. Unlabeled peaks due to SnS.

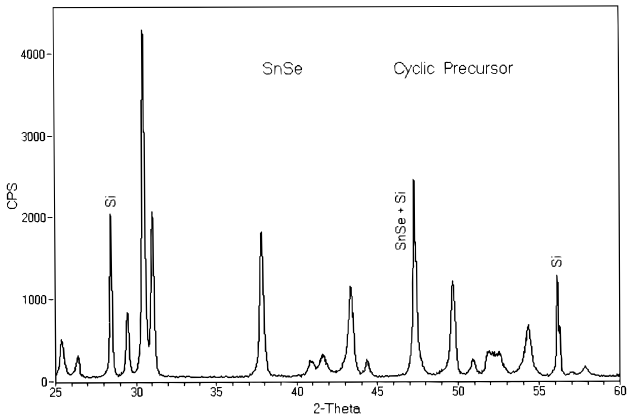

Figure 4. X-ray diffractogram of SnSe prepared from the pyrolysis of $(Bn_2SnSe)_3$. Silicon used as an internal *d*-spacing standard. Unlabeled peaks due to SnSe.

Table 2. XRD Measured Unit-Cell Parameters for SnS[a]

source	*a*, Å	*b*, Å	*c*, Å	vol, Å^3
PDF 33-1375	4.3340	11.2000	3.9870	193.53
PDF 39-354	4.3291(2)	11.1923(4)	3.9838(2)	193.03
DelBucchia[24]	4.329	11.180	3.982	192.72
Mossburg[25]	4.328	11.190	3.987	193.09
$(Ph_3Sn)_2S$[17]	4.3268(9)	11.1927(3)	3.9862	193.05
$(Ph_2SnS)_3$[16]	4.3184(12)	11.185(2)	3.9848(12)	192.48(6)
$(Bn_3Sn)_2S$ (**1**)	4.3259(5)	11.195(1)	3.9849(4)	192.97(2)
$(Bn_2SnS)_3$ (**2**)	4.3010(10)	11.209(2)	4.0001(6)	192.84(3)

[a] SnS, orthorhombic [GeS] structure type, space group *Pbnm*, $Z = 4$.

chalcogenides or, in the case of the linear precursors, the expected tin chalcogenide and elemental tin. No other crystalline phases, including oxides, were present, and no significant elevation of the background was observed to suggest any amorphous content.

Unit-cell analyses of the tin sulfide prepared by pyrolysis of the linear precursor **1** produced cell parameters that agree well with literature values, while the tin sulfide produced from the corresponding cyclic precursor **2** showed significant deviations from litera-

Table 3. XRD Measured Unit-Cell Parameters for SnSe[a]

source	*a*, Å	*b*, Å	*c*, Å	vol, Å^3
PDF 32-1382	4.46	11.42	4.19	213.4
Okazaki[26]	4.46	11.57	4.19	216.2
Nesterova[27]	4.47	11.48	4.19	215.0
Wiedemeier[28]	4.445	11.501	4.153	212.31
$(Ph_3Sn)_2Se$[17]	4.440(1)	11.4975(9)	4.1533(9)	212.03(4)
$(Ph_2SnSe)_3$[16]	4.418(1)	11.515(7)	4.170(1)	212.19(14)
$(Bn_3Sn)_2Se$ (**3**)	4.4422(4)	11.499(1)	4.1535(2)	212.18(3)
$(Bn_2SnSe)_3$ (**4**)	4.415(2)	11.513(3)	4.169(1)	211.96(5)

[a] SnSe, orthorhombic [GeS] structure type, space group *Pbnm*, $Z = 4$.

Table 4. XRD Measured Unit-Cell Parameters for Sn[a]

source	*a*, *b*, Å	*c*, Å	vol, Å^3
PDF 4-673	5.831	3.182	108.190
$(Bn_3Sn)_2S$	5.8319(2)	3.1816(1)	108.210(6)
$(Bn_3Sn)_2Se$	5.8315(2)	3.1816(2)	108.186(6)

[a] Sn, tetragonal [Sn] structure type, space group $I4_1/amd$.

ture values in its cell parameters (Table 2). The latter product exhibited a shorter *a* axis compensated by longer *b* and *c* axes to give a cell volume within the range of literature values. A similar trend was observed for tin selenide, with a shorter *a* axis and longer *b* and *c* axes in the $(Bz_2SnSe)_3$ pyrolysis product (Table 3), as compared to the product of **3**. Overall, the cell parameters of the SnS and SnSe prepared from cyclic benzyl precursors (**2** and **4**) most closely matched those observed in samples prepared from the cyclic phenyl precursors in our earlier work.[16]

It is interesting to note that a similar unit-cell transformation has been reported for tin sulfide above ambient temperatures.[23] Upon heating, tin sulfide transforms gradually towards the nearly tetragonal high temperature (>875 K) β form, with the *a* and *c* axes converging, and the *b* axis lengthening. During this transformation, the double layers assume a lesser distortion of the rocksalt structure, with atoms in the planes perpendicular to the *b* axis moving into square-planar coordination.[24] Our *a*-axis values for the products of **2** and **4** are consistent with literature values for the corresponding chalcogenides which were heated to approximately 560 K. This *a*-axis distortion is somewhat greater than observed for our *b*- and *c*-axis values (corresponding to literature values of material heated between roughly 350 and 450 K). While the individual cell dimensions were seen to deviate for **2** and **4** in the manner described, the resulting unit cell volumes agreed well with literature values.

The X-ray diffractograms of the powders resulting from the pyrolysis of $(Bn_3Sn)_2S$ and $(Bn_3Sn)_2Se$ confirm the presence of elemental tin mixed with the tin chalcogenide. The elemental tin has unit-cell parameters in excellent agreement with data reported for elemental tin by the National Institute of Standards and Technology (Table 4).

We note that the cyclic precursor produced powders with Bragg diffraction peaks on the order of 50% broader than corresponding reflections of the tin chalcogenides produced from the linear precursors. This indicates lower crystallinity of the tin chalcogenides prepared from the cyclic precursors relative to the products, which contained excess tin, obtained from the linear precursors. A marked decrease in crystallinity was noted for the (021) reflection, where a 3-fold increase in peak width (0.20° vs 0.60° 2θ) was observed in the samples from the cyclics. Clearly, the mechanisms involved in pyrolyzing the linear and cyclic precursors under identical conditions led to differing levels of crystalline order in the products.

The variations in unit cell parameters and crystallinity indicate that the pyrolysis products obtained from the linear and cyclic precursors differ. Although no sulfur, selenium or tin were detected in any of the pyrolysis byproducts, we cannot rule out the possibility that this is caused by slight differences in chemical composition from the ideal 1:1 ratio of tin to chalcogen. Albers et al. suggest the hole mobilities observed in their samples of SnS and SnSe (prepared by conventional heating of the elements in a sealed ampule) are due to tin vacancies.[8]

Thermogravimetric Analysis (TGA). The presence of elemental tin in the samples from the pyrolyses of **1** and **3** is particularly noteworthy. The resistance of tin to oxidation in combination with its electrical properties make it potentially useful in some thin film applications. Such films have been formed via the reduction of tin(II) chloride under a hydrogen atmosphere at temperatures of 400−500 °C.[29] An alternative route is the low pressure thermal decomposition of very light alkyl-substituted organotin compounds, such as tetramethyltin. This is done in the temperature range 500−600 °C.[30] Both methods require the deposition to take place well above the melting point of tin (232 °C). Thus, no practical applications have been found and it has been investigated only on an experimental basis.[15]

The benzyl-substituted tin compounds in this study show an onset of decomposition below 220 °C. The loss of mass appears as a single event and takes place over a narrow temperature range. No significant loss of mass is observed above 275 °C. GC/MS data showed small amounts of stilbene had formed in addition to the predominant byproduct of bibenzyl. It is likely that toluene had also formed as a minor byproduct. Thus, the onset temperature would be a better indication of the temperature at which the reaction actually begins. The relatively mild reaction temperatures suggest benzyl-substituted tin compounds may find use in a condensed (liquid) phase chemical deposition capacity. Experiments to this end are currently underway in this laboratory.

Sn (S_xSe_{1-x}) Solid Solutions. As noted above, SnS and SnSe are isostructural and capable of forming a continuous solid solution, with random substitution of S and Se at the chalcogen sites. Previous X-ray analysis of this solid solution series (produced by high-temperature solid-state techniques) showed the cell parameters to vary linearly across the range of chalcogen ratios.[8] XRD analysis of the products derived from mixing the cyclic precursors (**2** and **4**) in varying molar ratios prior to their pyrolysis confirm this linear solid solution

(23) Wiedemeier, H.; Csillag, F. J. *Z. Kristallogr.* **1979**, *149*, 17.
(24) DelBucchia, P. S.; Jumas, J. C.; Maurin, M. *Acta Crystallogr.* **1981**, *B37*, 1903.
(25) Mosburg, S.; Ross, D. R.; Bethke, M.; Toulmin, P. *U.S. Geol. Surv., Profess. Papers* **1961**, *424−C*, 347.
(26) Okazaki, A.; Ueda, I. *J. Phys. Soc. Jpn.* **1956**, *11*, 470.
(27) Nesterova, Y. M.; Pashinkin, A. S.; Novoselov, A. V. *Russ. J. Inorg. Chem.* **1961**, *6*, 1031.
(28) Weidemeier, H.; Csillag, F. *Z. Kristallogr.* **1979**, *149*, 17.
(29) Audosio, S. *J. Electrochem. Soc.* **1980**, *127*, 2299.
(30) Homer, H. J.; Cummins, O. U.S. Patent 2916400, 1959.

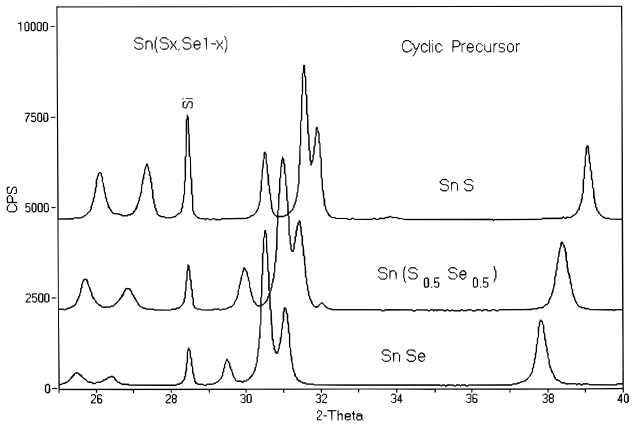

Figure 5. X-ray diffractograms of SnS, SnSe, and the solid solution $Sn(S_xSe_{1-x})$ at $x = 0.5$, all pyrolysis products of the cyclic precursors. Silicon used as an internal *d*-spacing standard.

Table 5. Lattice Parameters for SnS, SnSe, and Solid Solutions from 2 and 4

approximate composition of solid solution	*a*, Å	*b*, Å	*c*, Å	vol, Å^3
SnS	4.3010(10)	11.209(2)	4.0001(6)	192.84(3)
$Sn(S_{0.75}Se_{0.25})$	4.352(1)	11.304(2)	4.097(1)	199.10(6)
$Sn(S_{0.50}Se_{0.50})$	4.363(2)	11.387(2)	4.088(9)	203.09(7)
$Sn(S_{0.25}Se_{0.75})$	4.400(1)	11.468(3)	4.135(2)	208.62(9)
SnSe	4.415(2)	11.513(3)	4.169(1)	211.96(5)

behavior. No superstructure (which would be evidenced by extraneous weak reflections) or peak splitting was observed. The formation of a true solid solution is further supported by characteristic peak shifts observed in the XRD patterns from these samples (Figure 5) and analysis of the unit-cell parameters (Table 5). Figure 6 shows the variation of the unit-cell parameters as a function of the expected composition based upon the molar ratio at which the precursors, $(Bn_2SnS)_3$ and $(Bn_2SnSe)_3$, were combined. The variation is linear for the *a* and *c* axes. However, the long *b* axis shows a slight positive deviation from a linear dependence on composition, with a quadratic regression yielding an R^2 value of 0.999, compared to 0.986 for the linear regression of *b*. Figure 7 shows the unit-cell volume varies linearly with composition.

Phase Morphology. Electron micrographs of the powders show consistent and general platy habits. The samples obtained from the pyrolysis of precursor **1** consisted of small clusters of plates. The clusters were approximately 2−4 μm across. The individual plates are shown in Figure 8 to vary in size from 0.5 to 4 μm with a consistent thickness of approximately 0.25 μm. Figure 9 shows greater detail of the surface of these plates. Qualitative EDXRF analysis under SEM indicates the platy surfaces consist of tin and sulfur while point analysis of the smaller equiaxed particles on the surface detected primarily elemental tin. Similar morphology and composition were observed for the samples of SnSe and Sn obtained from the pyrolysis of **3**. The tin sulfide prepared from **2** shows the same general morphology characterized as clusters of plates approximately 2 μm across, each plate with a thickness of approximately 0.25 μm (Figure 10). The SnSe prepared from the pyrolysis of **4** consists of clusters approximately 1 μm across and also of the same thickness as the SnS samples (Figure 11). The 1:1 solid solution prepared

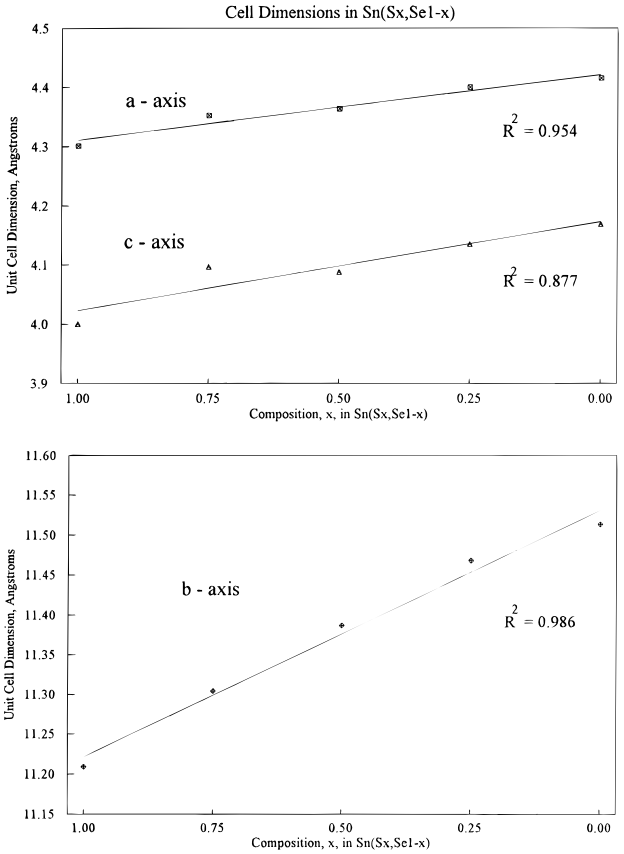

Figure 6. Unit cell dimensions in $Sn(S_xSe_{1-x})$. (A) Short (*a* and *c*) axes. (B) Long (*b*) axis. Compositions plotted are predicted values based on mixed ratios of the cyclic precursors prior to pyrolysis but are not believed to vary to a greater degree than the width of the plotted points.

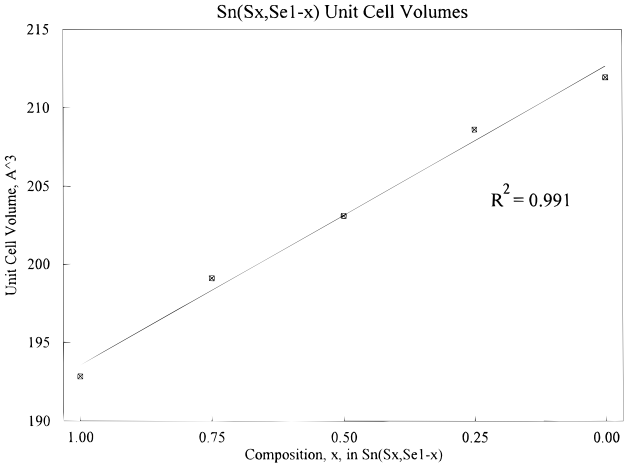

Figure 7. Unit-cell volumes in $Sn(S_xSe_{1-x})$. Pyrolysis product of cyclic precursors.

by combining the cyclic precursors (**2** and **4**) prior to their pyrolysis formed much larger clusters, up to 4 μm across. The dimensions of the individual plates are very close to those of the SnS sample (Figure 12).

Experimental Section

General Procedures. All reagents were purchased from Aldrich and, unless otherwise noted, were used without further purification. Selenium and organotin compounds are highly toxic and may be harmful by inhalation, ingestion, or skin absorption. Thus, protective clothing and gloves should be worn when handling them. All reactions and manipulations

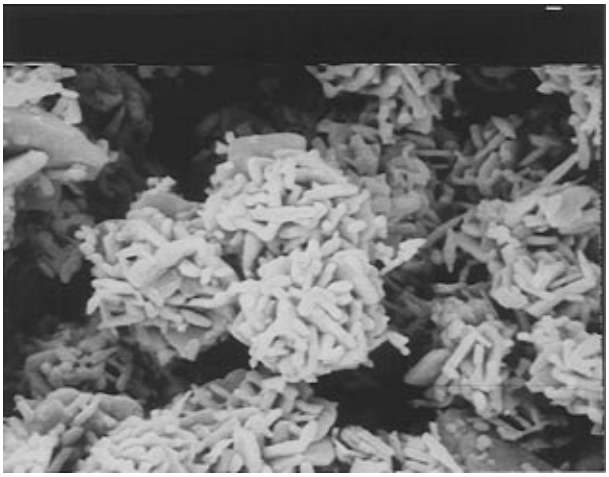

Figure 8. SEM (10 kV magnification 10 000×) of clusters of plates composed of SnS + Sn obtained from the pyrolysis of $(Bn_3Sn)_2S$.

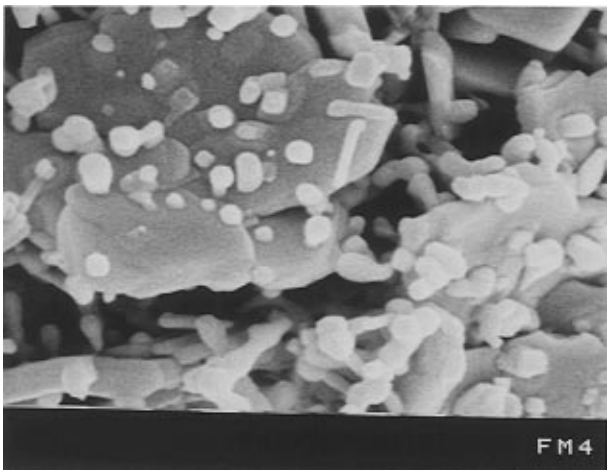

Figure 9. SEM (10 kV magnification 20 000×) of the surface of one of the plates comprising the clusters in the sample obtained from the pyrolysis of $(Bn_3Sn)_2S$.

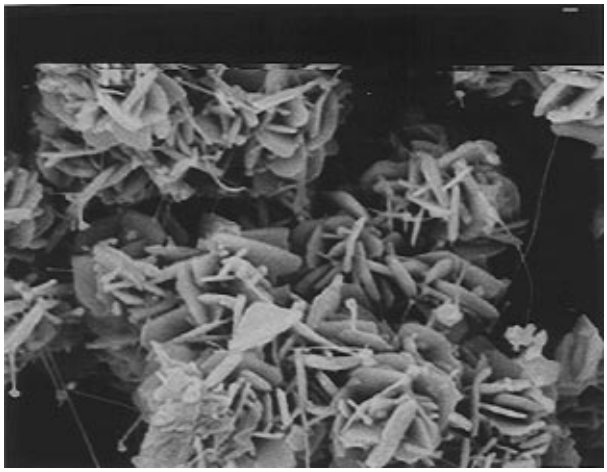

Figure 10. SEM (10 kV magnification 10 000×) of SnS obtained from the pyrolysis of $(Bn_2SnS)_3$.

were carried out in a fume hood. The benzyltin chloride compounds were prepared directly from tin powder and benzyl chloride using a slight variation of the procedure reported by Sisido et al.[31] Suspensions of sodium sulfide and sodium selenide were prepared immediately before use according to

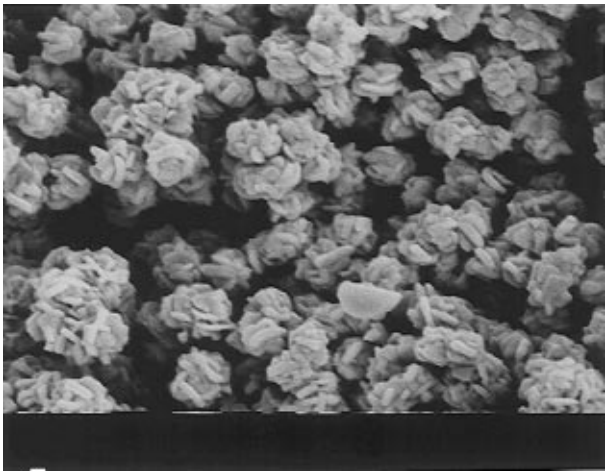

Figure 11. SEM (10 kV magnification 10 000×) of SnSe obtained from the pyrolysis of $(Bn_2SnSe)_3$.

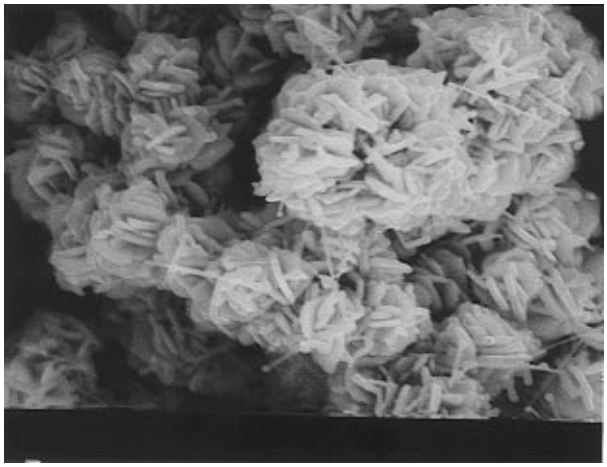

Figure 12. SEM (15 kV magnitification 10 000×) of Sn $(S_{0.5}$-$Se_{0.5})$ solid solution prepared by combining $(Bn_2SnS)_2$ and $(Bn_2$-$SnSe)_3$ prior to their pyrolysis.

literature procedures.[32,33] Tetrahydrofuran (THF) was distilled from sodium/benzophenone ketyl under a dry nitrogen atmosphere immediately before use. Toluene was distilled over sodium metal under a dry nitrogen atmosphere and stored over 3 Å molecular sieves prior to use.

Pyrolyses were carried out using a Lindberg Model 55035 programmable tube furnace, 36 cm long and 3 cm in diameter with a 55 × 2.5 cm Vycor silica glass tube placed inside. One end of the tube was fitted with a one-holed rubber stopper connected to a dry nitrogen source. Nitrogen flow was monitored at the exit of the tube by a mineral oil bubbler. The flow was set to approximately 50 mL/min and the tube was purged at this rate for at least 15 min prior to the introduction of the sample. The sample to be pyrolyzed was placed in a Coors porcelain boat which had been dried in an oven at 110 °C and cooled to room temperature in a desiccator. Typical sample size was 100−300 mg. The crucible containing sample was placed in the tube at the center of the furnace. For all samples, the oven was programmed to ramp at a rate of 10 °C/min to 125 °C, held at this temperature for 15 min to remove moisture and then ramped at a rate of 4 °C/min to 450 °C. This temperature was maintained for 2 h before allowing the oven to cool to room temperature. The volatile products condensed on the surface of the cooler regions of the tube and were collected.

NMR spectra were obtained on a JEOL GSX400 spectrometer at the following frequencies: ^{1}H (399.78 MHz), ^{13}C (100.52

(31) Sisido, K.; Takeda, Y.; Kinugawa, Z. *J. Am. Chem. Soc.* **1961**, *83*, 538.

(32) So, J. H.; Boudjouk, P. In *Inorganic Syntheses*; Grimes, R. N., Ed.; Wiley-Interscience: New York, 1992; Vol. 29, p 30.

(33) Thompson, D. P.; Boudjouk, P. *J. Org. Chem.* **1988**, *53*, 2109.

MHz), ^{119}Sn (148.99 MHz), and ^{77}Se (76.22 MHz). A 5-mm broad-band probe equipped with a variable-temperature accessory maintained the temperature at 25 ± 0.5 °C. Chemical shifts are reported in parts per million (ppm) from spectra taken of saturated solutions in $CDCl_3$ or CH_2Cl_2. ^{1}H and ^{13}C chemical shifts are reported with respect to Me_4Si (0 ppm). ^{119}Sn spectra were obtained using a pulse width of 15.0 μs, a pulse delay of 2.6 μs, and an acquisition time of 0.108 s. All ^{119}Sn shifts are relative to Me_4Sn in $CDCl_3$ (0 ppm). All ^{77}Se shifts are relative to a 25 % solution of Me_2Se in $CDCl_3$ (0 ppm). Spectra were obtained using a pulse width of 7.0 μs, a pulse delay of 3.3 μs, and an acquisition time of 0.134 s. To obtain acceptable signal to noise, up to 90 × 10^3 transients were required, depending upon sample solubility.

Thermogravimetric analysis (TGA) was done using a Perkin-Elmer 7 Series/UNIX Thermogravimetric Analyzer. The instrument was brought under control at 60 °C and scans were run at a ramp rate of 4 °C/min to 350 °C. The typical sample size was 5−12 μg. The onset of decomposition was calculated based upon a default trigger value of 1% of the starting sample mass. Gas chromatograph/mass spectrometer (GC-MS) analyses were carried out on a Hewlett-Packard 5880A Series GC-MS system equipped with a cross-linked methylsilicone capillary column. Melting points are uncorrected. Combustion analyses to determine residual carbon in the samples were performed by Galbraith Laboratories, Knoxville, TN. Scanning electron microscopy (SEM) was performed on a JEOL JSM 6300V instrument. The SEM samples were sputtered with gold to reduce charging effects.

X-ray powder diffraction (XRD) patterns were recorded from ethanol slurry-mounted samples on zero background quartz slides using a Philips automated vertical diffractometer with Cu Kα radiation from an AEG long fine-focus tube. The diffractometer setup included a θ-compensating variable divergence slit, a graphite diffracted beam monochromator, and a scintillation detector. Data reduction was performed on personal computers using MDI Jade software.[34] Unit-cell parameters were determined by the least-squares method, using the Garvey implementation of the Appleman and Evans code.[35] NIST SRM 640b silicon was used as an internal standard to ensure the accuracy of the cell parameters.

Synthesis of Dibenzyltin Dichloride. A 500 mL 3-necked round-bottomed flask was charged with tin powder (20.0 g, 169 mmol) and 250 mL of dry toluene and fitted with a condenser, a mechanical stirrer, and a 125 mL addition funnel containing benzyle chloride (19.4 mL, 17.6 g, 169 mmol). The suspension was stirred and heated to just below reflux. Distilled water (2 mL) was added through the condenser causing reflux. The benzyl chloride was added to this suspension over 10 min. Reflux was maintained for 4 h after which the hot solution was filtered to remove unreacted tin powder. Silky white crystals formed on cooling. The crystals were filtered and rinsed with cold toluene using a Büchner funnel. Yield: 22.6 g (72% based upon benzyl chloride) of dibenzyltin dichloride; mp 159−161 °C (lit.[32] 161−163 °C). Anal. Calcd for $C_{14}H_{14}SnCl_2$: C, 45.18%; H, 3.79%. Found: C, 45.18%; H, 3.79% NMR (270 MHz, $CDCl_3$) δ (^{1}H) 3.17 (s, CH_2); δ (^{13}C) 32.71 (CH_2); 126.76, 128.71, 129.56, 134.87 (Ar). ^{119}Sn NMR (400 MHz, $CDCl_3$): +26.3 ppm (lit.[36] +32.2 ppm). ^{119}Sn NMR (400 MHz, CH_2Cl_2): +36.0 ppm (lit.[37] +35 ppm).

Synthesis of Tribenzyltin Chloride. A 500 mL 3-necked round-bottomed flask, fitted with a condenser and a mechanical stirrer was charged with tin powder (25.0 g, 211 mmol) and 300 mL of distilled water. While stirring and heating to reflux, benzyl chloride (24.2 mL, 22.0 g, 211 mmol) was added through the condenser in 5 mL portions over 5 min. The reflux was maintained for 4 h which led to a solid gray mass of tin and soluble products. The mixture was filtered using a Büchner funnel. The solids were air dried and extracted with 300 mL of acetone for 4 h in a Soxhlet apparatus. The acetone was reduced to 50 mL using a rotary evaporator. Cooling this solution in an ice bath gave 23.1 g (77% based on benzyl chloride) of white crystals of tribenzyltin chloride: mp 142−145 °C (lit.[32] 142−144 °C). Anal. Calcd for $C_{21}H_{21}SnCl$: C, 59.00%; H, 4.95%. Found: C, 58.98%; H, 4.92% NMR (270 MHz, $CDCl_3$) δ (^{1}H) 2.73 (s, CH_2); δ (^{13}C) 25.08 (CH_2), 124.86, 127.76, 128.79, 137.91 (Ar). ^{119}Sn NMR (400 MHz, $CDCl_3$): +48.1 ppm (lit.[19] +52 ppm). ^{119}Sn NMR (400 MHz, CH_2Cl_2): +51.9 ppm (lit.[38] +53 ppm).

Synthesis of $(Bn_3Sn)_2S$ (1). A THF solution of Bn_3SnCl (11.1 g, 26.0 mmol in 30 mL of THF) was added to a freshly prepared suspension of sodium sulfide (13 mmol in 30 mL of THF) over 10 min. After an additional 10 h of stirring, this suspension was poured into 100 mL of water followed by extraction with five 50 mL portions of ether. The ether fractions were combined, dried over $MgSO_4$, filtered and the solvent reduced on a rotary evaporator until the solution became turbid. The flask was then placed in a freezer. After 10 h this produced 8.3 g (78 % yield) of white crystals of $(Bn_3Sn)_2S$ (**1**): mp 83−85 °C. Anal. Calcd for $C_{42}H_{42}Sn_2S$: C, 61.86%; H, 5.19%. Found: C, 61.51%; H, 5.27%. NMR (270 MHz, $CDCl_3$) δ (^{1}H) (s, CH_2); δ (^{13}C) (CH_2), 124.86, (Ar), ^{119}Sn NMR ($CDCl_3$): +26.1 ppm (lit.[38] +26.9 ppm).

Synthesis of $(Bn_3Sn)_2Se$ (2). A solution of Bn_3SnCl (11.1 g, 26.0 mmol in 40 mL of THF) was added to a freshly prepared suspension of sodium selenide (13 mmol in 30 mL of THF) over a 10 min period. The white suspension turned light brown after the addition and darkened to black after several hours. The reaction was allowed to stir for an additional 10 h. The product was worked up in the same fashion as **1** to give 9.8 g (88% yield) of $(Bn_3Sn)_2Se$ (**2**): mp 60−63 °C. Anal. Calcd for $C_{42}H_{42}Sn_2Se$: C, 58.50%; H, 4.91%. Found: C, 58.38%; H, 4.89%. NMR (270 MHz, $CDCl_3$) δ (^{1}H) 2.50 (s, CH_2); δ (^{13}C) 24.71 (CH_2): 124.88, 128.29, 129.19, 140.34 (Ar). ^{119}Sn NMR (400 MHz, $CDCl_3$): −2.4 ppm (lit.[39] 2.0 ppm). ^{77}Se NMR (400 MHz, $CDCl_3$): −542.36 ppm.

Synthesis of $(Bn_3SnS)_3$ (3). A solution of Bn_2SnCl_2 (8.0 g, 22 mmol in 30 mL of THF) was added to a freshly prepared suspension of sodium sulfide (22 mmol in 50 mL of THF) at room temperature over 15 min. The white suspension turned light brown after 4 h of stirring at room temperature. The product was worked up in the same fashion as **1** to give 6.2 g (85%) of $(Bn_2SnS)_3$ (**3**): mp 182−185 °C. Anal. Calcd for $C_{42}H_{42}Sn_3S_3$: C, 50.54; H, 4.24%. Found: C, 50.41%; H, 4.45%. NMR (270 MHz, $CDCl_3$) δ (^{1}H) 2.71 (s, CH_2); δ (^{13}C) 31.12 (CH_2); 125.57, 128.61, 129.13, 138.28 (Ar). ^{119}Sn NMR (400 MHz, $CDCl_3$): +76.1 ppm.

Synthesis of $(Bn_3SnSe)_3$ (4). A solution of Bn_2SnCl_2 (8.0 g, 22 mmol in 30 mL of THF) was added to a freshly prepared suspension of sodium selenide (22 mmol in 50 mL of THF) over 15 min. The white suspension turned light brown after 4 h of stirring at room temperature. The product was worked up in the same fashion as **1** to give 7.9 g (97 % of $(Bn_2SnSe)_3$ (**4**): mp 155−157 °C. Anal. Calcd for $C_{42}H_{42}Sn_3Se_3$: C, 44.32%; H, 3.72%. Found: C, 44.24%; H, 3.71%. NMR (270 MHz, $CDCl_3$) δ (^{1}H) 2.81 (s, CH_2); δ (^{13}C) 30.02 (CH_2); 124.99, 128.08, 128.64, 138.25 (Ar). ^{119}Sn NMR (400 MHz, $CDCl_3$): 14.7 ppm. ^{77}Se NMR (400 MHz, $CDCl_3$): −372.49 ppm.

Conclusions

In our earlier work we investigated phenyl substituted tin chalcogen molecules as precursors to SnS, SnSe, and SnTe.[16−18,40] We noted several advantages to these precursors. They are easily synthesized and are air and moisture stable. Their high molecular

(34) Materials Data Incorporated. *Jade + S/M v2.1* Livermore, CA, 1988−94.

(35) (a) Garvey, R. G. *Powder Diffraction*, **1986**, *1*, 114. (b) Appleman, D. E.; Evans, H. T. *U.S. Geological Survey Report PB 216188*; U.S. Dept. of Commerce, Nat. Tech. Info. Serv.

(36) Holeček, J.; Lyčka, A.; Handlíř, K.; Nádvorník, M. *Coll. Czech. Chem. Commun.* **1988**, *53*, 571.

(37) Verdonck, L.; Van der Kelen, G. P. *J. Organomet. Chem.* **1972**, *40*, 139.

(38) Kerschl, S.; Wrackmeyer, B. *Z. Naturforsch.* **1987**, *42b*, 387.

(39) Wrackmeyer, B. *Annu. Rep. NMR Spectrosc.* **1985**, *16*, 73.

(40) Seidler, D. J.; Boudjouk, P.; Bahr, S. R.; McCarthy, G. J. *206th National Meeting of the American Chemical Society*; Chicago, IL, August 22−27, 1993; Abstract INOR 166.

weights make them less of a health hazard. These features are common with the benzyl analogues of those compounds investigated here. However, unlike phenyl groups, which migrate upon pyrolysis to yield tetraphenyltin and diphenyl chalcogenide byproducts, we observe a free-radical mechanism in which all of the benzyl tin bonds break leading to the formation of bibenzyl as the only byproduct. The pyrolysis products from the cyclic molecules **2** and **4**, SnS and SnSe, respectively, were XRD phase pure. The linear precursors (**1** and **3**) give a mixture of the tin chalcogenide and elemental tin upon pyrolysis. Detailed analyses of the SnS and SnSe X-ray diffractograms and unit-cell parameters indicate that the linear and cyclic precursors, pyrolyzed under identical conditions, yield products of different crystallinity and probably different stoichiometry.

A single volatile organic compound as the only byproduct, which contains all atoms other than the metal and chalcogen atoms incorporated in the target material, is an important feature of these systems. Higher ceramic yield, low carbon contamination, and excellent control over the stoichiometry of the metal chalcogenide are the most critical advantages over more complex systems. It is an added benefit that the perbenzylated precursors can be prepared on large scale in a straightforward fashion.

It was also demonstrated that $(Bn_2SnS)_3$ and $(Bn_2SnSe)_3$ can be used effectively to synthesize solid solutions in a single step. These organometallic precursors are easily combined in any desired ratio. They apparently mix effectively at the molecular level in the melt phase prior to decomposition leading to a one-step low-temperature preparation of ternary phases.

These results suggest that the largely uninvestigated benzyl group has excellent potential for serving as a leaving group in numerous other applications. We recently reported the use of this strategy in the preparation of bulk samples of $SnSe_2$ and ultrafine particles of SnS_2.[41]

Acknowledgment. Financial support from the Air Force Office of Scientific Research through Grant No. F49620-92-J-0431 and the National Science Foundation through Grant OSR 9452892 is gratefully acknowledged. We also thank Dr. Thomas Freeman and Kathy Iverson for assistance with the SEM characterization.

CM9504347

(41) Seidler, D. J.; Boudjouk, P.; Grier, D. G.; McCarthy, G. J. *210th National Meeting of the American Chemical Society*; Chciago, IL Aug 20−24, 1995; Abstract INOR 513.